

The influence of the tangential velocity of inner rotating wall on axial velocity profile of flow through vertical annular pipe with rotating inner surface

Abdusalam M. Sharf^{1,a}, Hosen A. Jawan¹ and Fthi A. Almabsout¹

¹Mechanical Department Faculty of Engineering, Elmergib University, Alkhoms, Libya

Abstract. In the oil and gas industries, understanding the behaviour of a flow through an annulus gap in a vertical position, whose outer wall is stationary whilst the inner wall rotates, is a significantly important issue in drilling wells. The main emphasis is placed on experimental (using an available rig) and computational (employing CFD software) investigations into the effects of the rotation speed of the inner pipe on the axial velocity profiles. The measured axial velocity profiles, in the cases of low axial flow, show that the axial velocity is influenced by the rotation speed of the inner pipe in the region of almost 33% of the annulus near the inner pipe, and influenced inversely in the rest of the annulus. The position of the maximum axial velocity is shifted from the centre to be nearer the inner pipe, by increasing the rotation speed. However, in the case of higher flow, as the rotation speed increases, the axial velocity is reduced and the position of the maximum axial velocity is skewed towards the centre of the annulus. There is a reduction of the swirl velocity corresponding to the rise of the volumetric flow rate.

1 Introduction

In the oil and gas industries, the drilling fluids play the main role in oil and gas drilling. Following the success of the first rotary drilling well, the technology of the drilling well became significantly important. Nowadays, much attention has been paid on developing the technology of drilling and drilling fluids. One of the main and most important functions of the drilling fluids is the cutting removal from the borehole; the cuttings generated by the bit must be removed immediately to achieve an effective drilling process [1].

Several factors influence the carrying capacity of the drilling fluids, such as annulus velocity, plastic viscosity and yield point of the mud and slip velocity of the generated cuttings. For a cutting to reach the surface, the slip velocity must be lower than the average annular velocity. As an approximate guide, the minimum annular velocities for hole sizes of 15, 12.5, 10.623, 8.75, 7.875 and 6 inches are 80, 90, 110, 120, 130 and 140 ft/min, respectively [2].

This research aims to investigate the characteristics of tangential and axial velocities of flow in a vertical concentric annulus, whose outer cylinder is stationary and inner cylinder is rotating. In order to accomplish this aim, an experiment and numerous calculations have been performed. Furthermore, data collected from these approaches will be compared to investigate the effect of

swirl velocity on the axial velocity profile, and how well the computation predicts this flow:

- Experimental approach: experimental data will be collected by using a rig that is available in the Fluid Dynamics Lab at Newcastle University.
- Numerical approach: calculated data based on Computational Fluid Dynamics (CFD) software Gambit and FLUENT. This approach is widely accepted for engineering problems, as it is reliable, cost effective and less time consuming.

1.2 Computational fluid dynamics (CFD)

The last two decades have seen very rapid growth in the understanding of computational fluid dynamics, or CFD modeling, which is extensively used to predict and analyze the behaviour of fluid flows. “CFD is the analysis of the systems involving fluid flow, heat transfer and associated phenomena such as chemical reactions by means of computer-based simulation” [3].

Since CFD is powerful, it spans a wide range of industrial and non-industrial applications, and an example of these applications is the flow through an annulus pipe. “[a]nnular pipe flow is important in engineering applications such as heat exchangers, gas-cooled nuclear reactors and drilling operations in the oil and gas industry”[4]. They studied a turbulent concentric annular

^a sharf762001@yahoo.com

pipe flow for two radius ratios ($R1/R2=0.1$ and 0.5), by using the direct numerical simulation.

Experimental and numerical studies have been done on fully developed turbulent flow through concentric annuli (Knudsen and Katz, 1950; Brighton and Jones, 1964; Quarmby, 1967; Rehme, 1974). The radial positions between zero shear stress and maximum velocity were the main focus on these studies. It was reported by Knudsen and Katz (1950), Brighton and Jones (1964), and Quarmby (1967) that the radial location of maximum velocity is synchronized with the location of zero shear stress. However, Rehme (1974) remarked that the position of zero shear stress is closer to the inner wall than maximum velocity. An LDV experiment in concentric annuli was conducted by Nouri et al (1993) and Escudier et al (1995)[4].

A lot of studies have been done about flow through the tube and annulus pipe, but far too little attention has been paid to flow through the annulus pipe with rotation of the inner wall. However, a study of flow through an annulus with rotating the inner cylinder was done by Nouri and Whitlaw (1994) [5].

The latest study on this problem was done by Essiwi (2006), to investigate the validity of CFD modeling for oil well drilling fluid flows; he considered the axial and swirl velocities as they affect the process of lifting the generated cuttings[2].

2 Experimental model

The experimental measurements were established by using the rig available (fig 2.1) to measure the axial and swirl velocities of the flow through the vertical annular pipe, whilst rotating the inner one. The velocities will be measured by using a Laser Doppler Velocimeter (LDV) at different distances from the inner pipe. The measurements were taken at 1.4 m from the bottom of the module, because at this location, the axial velocity is fully developed [2].

The axial flow through the annulus give axial Reynolds numbers in the range of $Re_Q=0$ (zero flow rate), $Re_Q \approx 4 \times 10^3$ (low flow rate) and $Re_Q \approx 1 \times 10^4$ (high flow rate) that calculated from equation (2.1). The rotation speeds of the inner pipe were taken 75, 150, 225 and 300 rev/min with zero, low and high flow rate.

$$Re_Q = \frac{Q}{\nu D \left(1 + \frac{d_e}{D} \right)} \quad (2.1)$$

Also, from equation (2.2), rotational Reynolds numbers are $Re_\omega = 0$, $Re_\omega = 28 \times 10^3$, $Re_\omega = 66 \times 10^3$, $Re_\omega = 85 \times 10^3$ and $Re_\omega = 11 \times 10^4$.

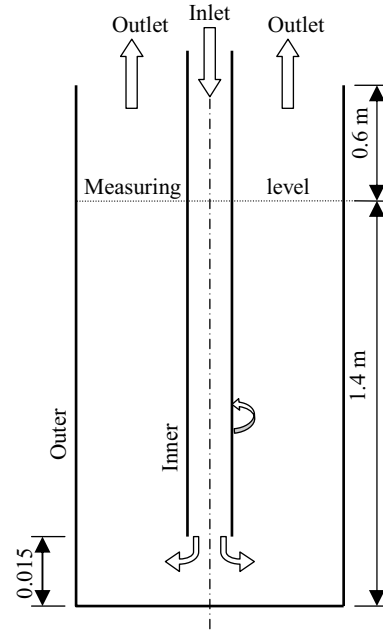


Figure 2.1. Physical experimental model

$$R_\omega = \frac{\omega \times (d_e)^2}{\nu} \quad (2.2)$$

3 Turbulence and its modelling

3.1 Turbulent model

In this study, two-equation models are used which is standard $k - \epsilon$ model, and for simplification reasons, the geometry is solved as two-dimensional axisymmetric simulation. Fluid flows are usually unsteady, three-dimensional and involve fluids that are to some degree compressible. Many simplifying assumptions are frequently made, for example that the flow is steady or restricted to less than three dimensions, or that it is practically incompressible [6].

The standard $k - \epsilon$ is a semi-empirical model which has become the workhorse of practical engineering flow calculations in the time since it was proposed by Launder and Spalding (1972) [7]. The model is based on model transport equations for the turbulent kinetic energy, k , and its dissipation rate, ϵ . The turbulent viscosity is computed from these scalars. The $k - \epsilon$ formulation is derived using a high Reynolds number hypothesis; also, near wall treatment is based on the application of wall functions, rather than solving governing equations inside the boundary layer.

3.2 Boundary conditions

Figure 3.1 shows the boundary conditions for the computational solution domain, as the outlet is open to atmospheric pressure, radial equilibrium pressure

distribution and zero gauge pressure were set in the pressure outlet panel. The outer wall and the bottom were set as stationary walls with no-slip conditions. The inner wall was set as a moving wall with a specified rotation speed (0, 75, 150, 225 and 300rev/min). The working fluid is water with software default parameters (density of 998.2 kg/m³ and viscosity of 100.3×10⁻⁵ kg/ms).

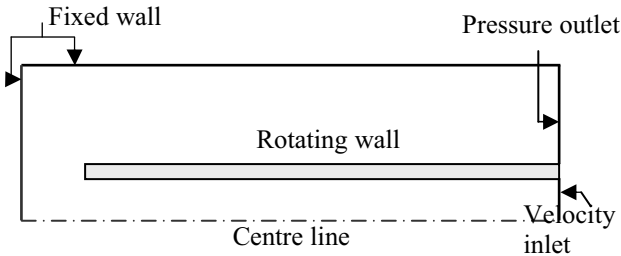


Figure 3.1. The boundary conditions of the geometry

3.2.1 y^+ for the meshes used

The y^+ values of the mesh used with standard model were checked and are shown in figure 3.2 (a)-(d). y^+ values for the mesh are in the appropriate range ($y^+ \approx 1$). Since the focus in this study is not on the flow in the inner pipe, thus the mesh close the inner surface of the rotating wall is not as fine as in the annulus. Therefore, for the inner surface of the rotating wall, high values of y^+ are shown in fig 3.2.

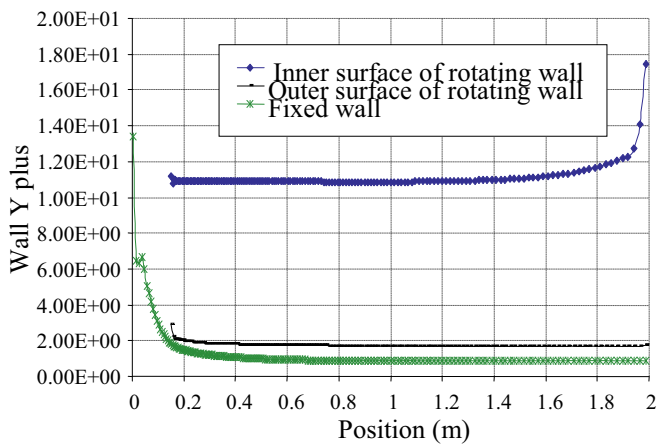


Figure 3.2. y^+ for standard $k - \epsilon$ model.

4 Results and discussion

4.1 Comparisons for measured and computed results

Figure 4.1- 4.4 indicate measured and computed results.

Figure 4.1(a) and (b) show comparisons between the profiles of axial velocity for zero rotation speed of the inner pipe with volumetric flow rate of 0.994 and 2.68 l/s respectively. The standard $k - \epsilon$ model gives good agreement between experimental and computational profiles with low axial flow rate (0.994 l/s), but not at the high flow rate (2.68 l/s).

The profiles obtained by the standard $k - \epsilon$ model with high volumetric flow rate, shows the maximum velocity near the inner pipe, whereas it is towards the middle of the annulus in the experimental profiles. In figure 4.1 (a) and (b), particularly close to the outer wall, the experimental results have uncertainties due to reflection from the wall.

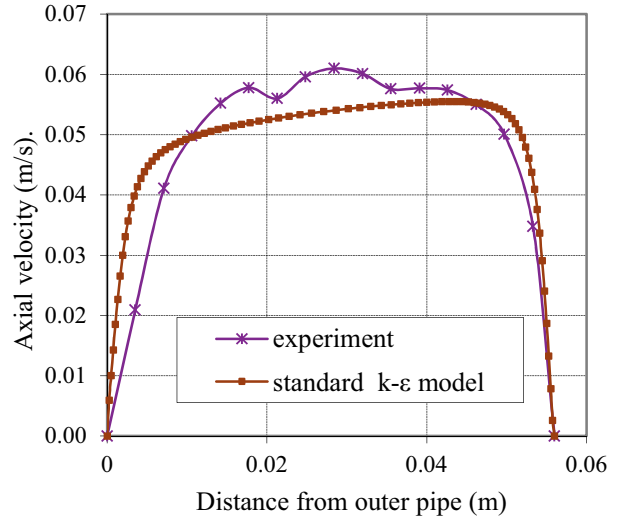


Figure 4.1 (a). Comparison between experimental and computational axial velocity profiles at inner pipe rotation speed of 0rev/min and volumetric flow rate of 0.994 l/s.

Measured and computed profiles of axial and swirl velocities are shown in fig 4.2 (a) and (b), respectively, in the case of rotating the inner pipe at 225rev/min with zero axial flow rate. Fig 4.2 (a) shows a general shape of computed axial velocity profiles.

The magnitudes of the measured axial velocity are from -0.012 to 0.01m/s, but as this indicates a net outflow, the measured and computed profiles are close to each other near the outer wall up to 40% of the annulus gap, but then they diverge towards the inner pipe.

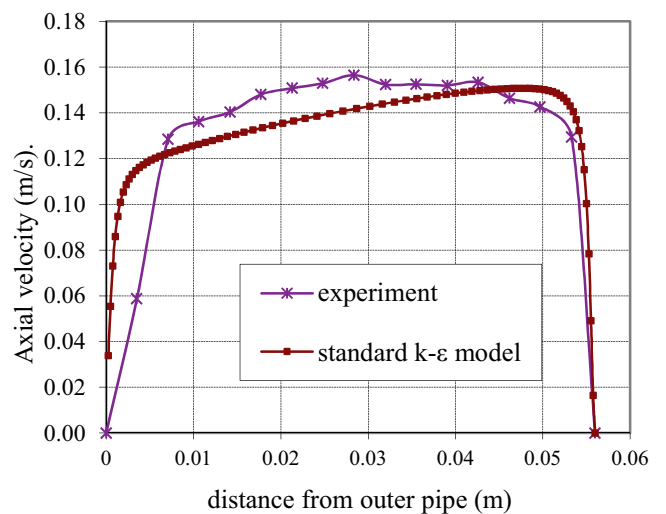


Figure 4.1 (b). Comparison between experimental and computational axial velocity profiles at inner pipe rotation speed of 0rev/min and volumetric flow rate of 2.68 l/s.

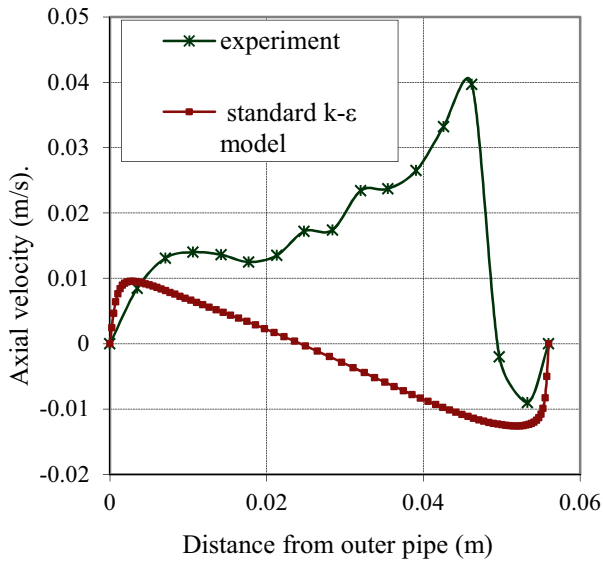


Figure 4.2 (a). Comparison between experimental and computational axial velocity profiles at inner pipe rotation speed of 225rev/min and zero volumetric flow rate.

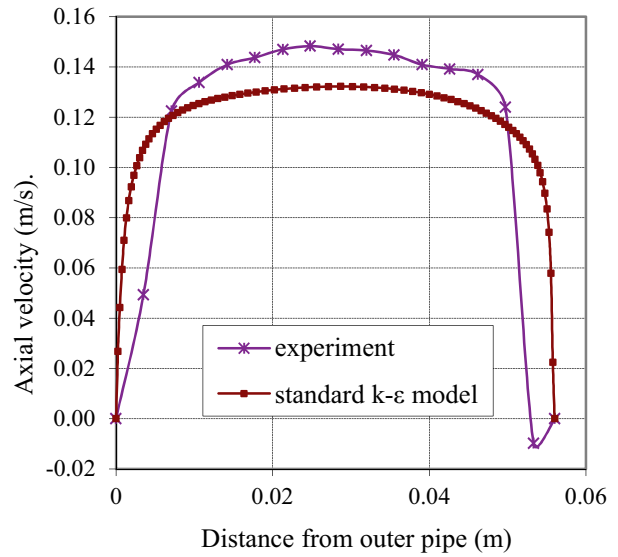


Figure 4.3 (a). Comparison between experimental and computational axial velocity profiles at inner pipe rotation speed of 225rev/min and volumetric flow rate of 2.467 l/s.

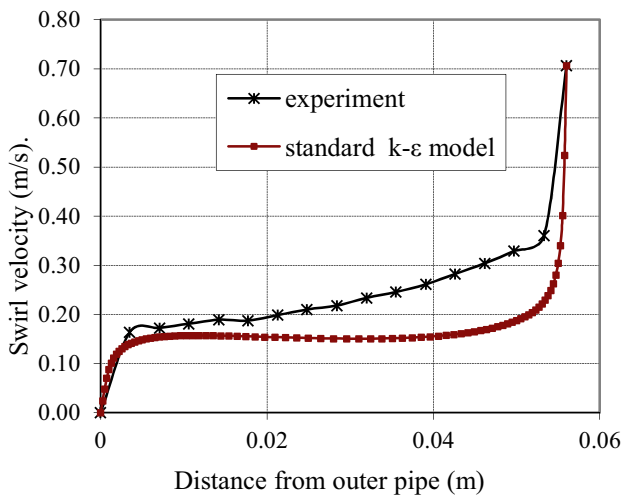


Fig 4.2 (b). Comparison between experimental and computational swirl velocity profiles at inner pipe rotation speed of 225rev/min and zero volumetric flow rate.

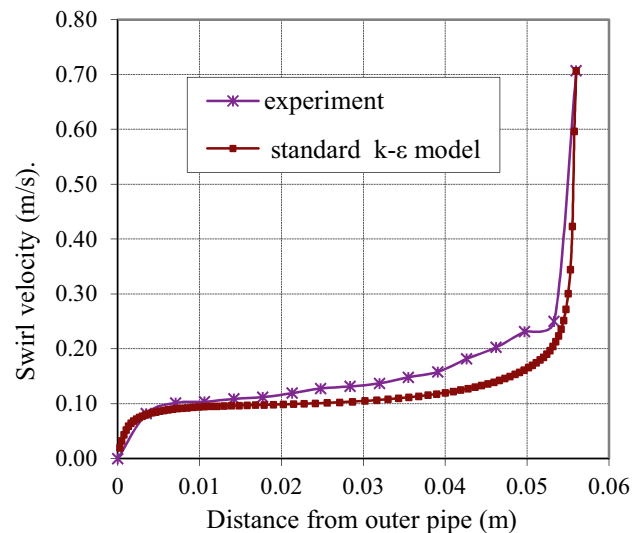


Figure 4.3 (b). Comparison between experimental and computational swirl velocity profiles at inner pipe rotation speed of 225rev/min and volumetric flow rate of 2.467 l/s.

A comparison of measured and computed axial velocity profiles is shown in fig 4.3 (a), which shows the case of rotating the inner pipe at 225rev/min, with a volumetric flow rate of 2.467 l/s. The shape of these profiles is similar to that in fig 4.7 (75rev/min and high axial flow rate 2.43 l/s). The model used does not indicate the maximum values of axial velocity given by the measured profile. The odd shape of the measured profile close to the inner pipe is probably due to the measurements' uncertainty.

Figure 4.3 (b) indicates the corresponding comparison for the swirl velocity profiles for the inner pipe rotation speed of 225rev/min with axial flow rate of 2.467 l/s. There is some agreement between experimental and computational profiles.

Figures 4.4 (a) and (b), with rotation speed of the inner pipe at 225rev/min and volumetric flow rate of 0.921 l/s, show the measured and computed profiles of axial and swirl velocities, respectively. The model used can not predict the maximum value, yet by contrast to the experiment, the profile obtained by standard model shows that the maximum values of the axial velocity is shifted towards the outer wall.

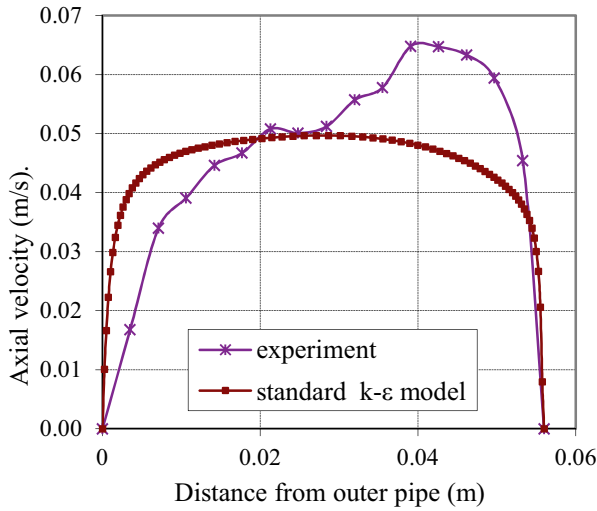


Figure 4.4 (a). Comparison between experimental and computational axial velocity profiles at inner pipe rotation speed of 225rev/min and volumetric flow rate of 0.921 l/s.

Figure 4.4 (b) presents a comparison for swirl velocity profiles which shows some agreement with experimental data, although a deviation is observed in the region of a <0.04m distance from the outer wall. The shape of the profiles in fig 4.4 (b) is similar to that in fig 4.3 (b).

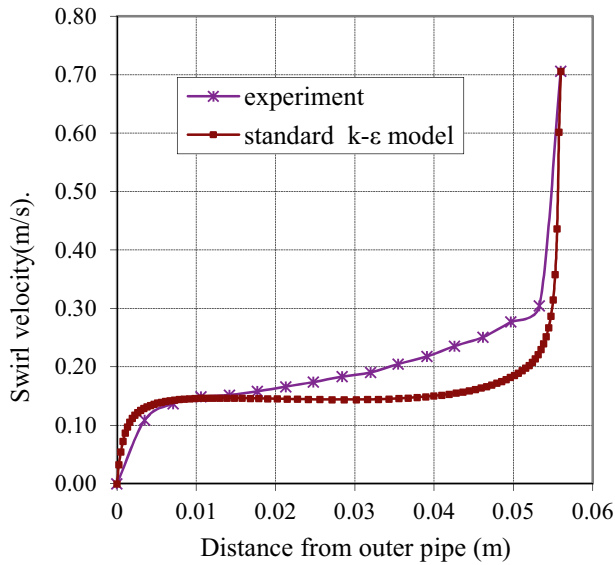


Figure 4.4 (b). Comparison between experimental and computational swirl velocity profiles at inner pipe rotation speed of 225rev/min and volumetric flow rate of 0.921 l/s.

4.2 The behaviour of the computed axial velocity profiles as the rotation speeds of the inner pipe increases

Profiles of measured axial velocity in the cases of zero volumetric flow rate with different rotation speeds of the inner pipe (150, 225 and 300rev/min) are shown in figure 4.5. The axial velocity is directly proportional to the rotation speed, and the absolute magnitude of the axial

velocity in the inner region of the annulus gap is higher than in the outer region. The positions of the zero value of the axial velocity in three cases are skewed to the outer wall, rather than the middle of the annulus, at about 0.024m away from the outer wall. Again, the rotation speed of the inner pipe generates a re-circulating flow into the annulus.

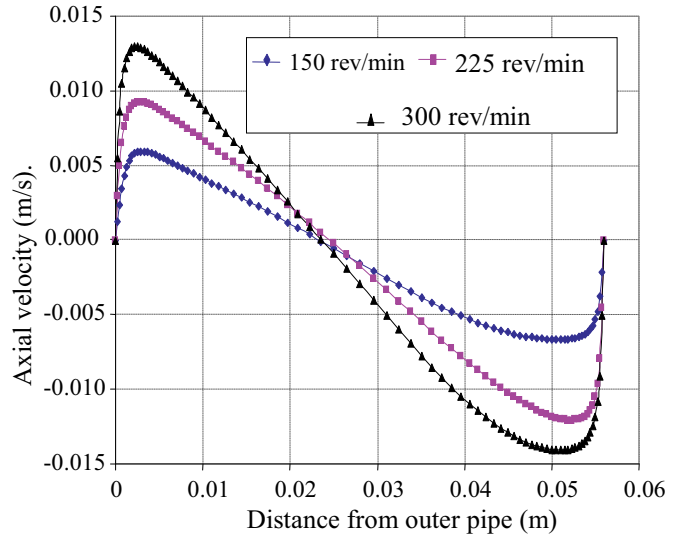


Figure 4.5. Comparison of computed axial velocity profiles for three different rotational speeds of the inner pipe, for $Re_Q = 0$.

Figure 4.6 shows the axial velocity profiles in cases of rotation speeds of the inner pipe at zero, 225 and 300rev/min for $Re_Q = 4 \times 10^3$. In figure 4.6, as the rotation speed increases, the axial velocity reduces; this influence of the rotation speed on the axial profiles is clearly seen at the outer region. However, in the inner region, from 0.037 to 0.056m away from the outer pipe, a similar influence is seen up to 225rev/min, and then the axial velocity increases as the rotation speed increases.

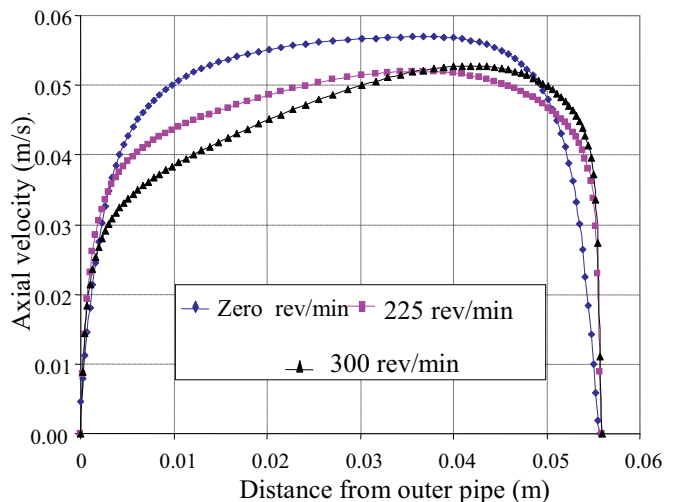


Figure 4.6. Comparison of computed axial velocity profiles for three different rotational speeds of the inner pipe, for $Re_Q = 4 \times 10^3$.

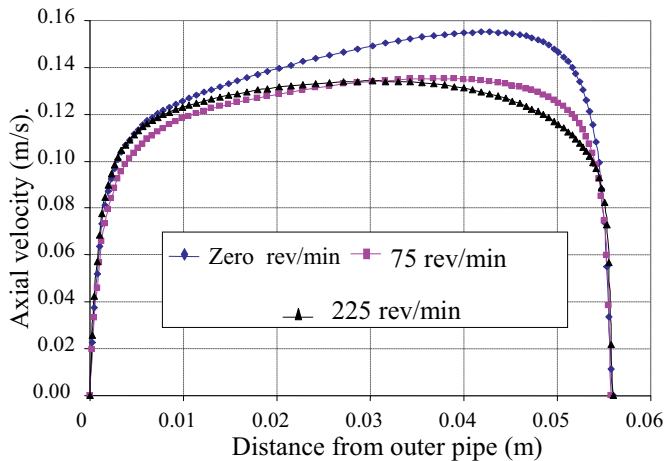


Figure 4.7. Comparison of computed axial velocity profiles for three different rotational speeds of the inner pipe, for $Re_Q = 1 \times 10^4$.

In the inner half of the annulus, it is obvious that the axial velocity is a function of the rotation speed (inversely proportional to the rotation speed). On the other hand, in the outer half, the axial velocity reduces as the rotation speed increases up to 75 rev/min, and then the axial velocity increases. Completely different from the profiles in figure 4.6, in figure 4.7, the profile of the axial velocity becomes flatter as the rotation speed increases. In general, from figure 4.6 and 4.7, for rotation speeds ≤ 225 , the axial velocity decreases as the rotation speed of the inner pipe increases.

5 Conclusion

1. The experimental velocity profiles were obtained by using the rig which measures the axial and swirl velocities, by using a Laser Doppler Velocimeter (LDV).
2. Measurement uncertainties were seen close to the walls of the annulus gap, especially near the rotating wall, due to laser reflection and orbit motion of the inner pipe, which was assumed to be neglected.
3. The measured swirl velocity profile is directly proportional to the rotation speed. However, the axial flow rate influences this relation, namely, the effect of the rotation speed is reduced by the increase of the axial flow rate.
4. Axial profiles show the value of zero at the outer wall, which corresponds to the on-slip condition at the outer wall and the value of the inner pipe tangential velocity. A sudden increase in the swirl velocity is shown in the region very close to the outer wall, and then the axial velocity steadily increases towards the inner pipe and a rapid increase is again shown nearer the inner wall.

5. Comparisons between computational and experimental results showed that the calculations predicted the qualitative features of the axial and swirl velocity profiles to be satisfactory.
6. Computed axial velocity profiles show good agreement with corresponding measurements in the case of a stationary inner pipe. Similar agreements are shown by the swirl profiles for rotation speeds ≤ 75 rev/min. On the other hand, for high rotation speeds, and in the region above 30% away from the outer wall, except very close the inner pipe, the computed swirl profiles show smaller values than the measured one.
7. The computed axial velocity profiles do not indicate the maximum measured axial velocity when the rotation speed increases. Also, a discrepancy between the measured and computed profiles of the axial velocity is probably due to the measurements errors, rather than the predictive inabilities of the calculations.

References

1. G.Reich, H. Beer, International Journal of Heat and Mass Transfer, **32**: 551-562 (1989)
2. M. M. Essiwi, *Validation of CFD Modeling for Oil Well Drilling Fluid Flow*. PhD Thesis, University of Newcastle upon Tyne, Newcastle upon Tyne (2006)
3. H. K.Versteeg, W. Malalasekera, *Computational Fluid Dynamics the Finite Volume Method 2nd edn*. Prentice Hall, Harlow (2007)
4. S. Chung, International Journal of Heat and Fluid Flow, **23**:426-440 (2002)
5. M. Nouri, Journal of Fluid Mechanics Digital Archive, **253**: 617-641 (1993)
6. M. B. Aboott, B. R. Basco, *Computational Fluid Dynamics an introduction for Engineers*. Longman, Harlow (1989)
7. Fluent. Inc. (2001). Fluent 6.0 Users Guide, Dec. 2001. 5 Vols, Fluent Inc, Lebanon NH, USA.